

# Putty-like bone fillers based on CaP ceramics or Biosilicate<sup>®</sup> combined with carboxymethylcellulose: Characterization, optimization, and evaluation

Paulo R Gabbai-Armelin<sup>1,2,3</sup>, Ana CM Renno<sup>1</sup>, Murilo C Crovace<sup>4</sup>, Angela MP Magri<sup>1,2</sup>, Edgar D Zanotto<sup>4</sup>, Oscar Peitl<sup>4</sup>, Sander CG Leeuwenburgh<sup>2</sup>, John A Jansen<sup>2</sup> and Jeroen JJP van den Beucken<sup>2</sup>

## Abstract

Calcium phosphates and bioactive glass ceramics have been considered promising biomaterials for use in surgeries. However, their moldability should be further enhanced. We here thereby report the handling, physicochemical features, and morphological characteristics of formulations consisting of carboxymethylcellulose–glycerol and hydroxyapatite-tricalcium phosphate or Biosilicate<sup>®</sup> particles. We hypothesized that combining either material with carboxymethylcellulose–glycerol would improve handling properties, retaining their bioactivity. In addition to scanning electron microscopy, cohesion, mineralization, pH, and viscoelastic properties of the novel formulations, cell culture experiments were performed to evaluate the cytotoxicity and cell proliferation. Putty-like formulations were obtained with improved cohesion and moldability. Remarkably, mineralization in simulated body fluid of hydroxyapatite-tricalcium phosphate/carboxymethylcellulose–glycerol formulations was enhanced compared to pure hydroxyapatite-tricalcium phosphate. Cell experiments showed that all formulations were noncytotoxic and that HA-TCP60 and BGC50 extracts led to an increased cell proliferation. We conclude that combining carboxymethylcellulose–glycerol with either hydroxyapatite-tricalcium phosphate or Biosilicate<sup>®</sup> allows for the generation of moldable putties, improves handling properties, and retains the ceramic bioactivity.

## Keywords

Bone augmentation, calcium phosphates, ceramic granulate, carboxymethylcellulose–glycerol, bone repair

## Introduction

Bone augmentation is a surgical procedure aiming to reconstruct atrophic regions prior to implant placement.<sup>1</sup> For this purpose, autografts, allografts, xenografts, and alloplasts are used as treatment options.<sup>2</sup> Major efforts have been dedicated to developing appropriate materials for bone augmentation. Considering this matter, two different classes of biomaterials—calcium phosphates (CaP) and bioactive glasses/glass ceramics (BG/BGC)—have been considered promising synthetic materials for use in orthopedic and craniomaxillofacial surgery due to their excellent biocompatibility and bioactivity.<sup>3–6</sup> These biomaterials generate a particular biological response

<sup>1</sup>Laboratory of Biomaterials and Tissue Engineering, Department of Biosciences, Federal University of São Paulo, Santos, Brazil

<sup>2</sup>Department of Biomaterials (309), Radboudumc, Nijmegen, The Netherlands

<sup>3</sup>Department of Physiotherapy, Biotechnology Post-graduate Program, Federal University of São Carlos, São Carlos, Brazil

<sup>4</sup>Vitreous Materials Laboratory (LaMaV), Department of Material Engineering, Federal University of São Carlos, Sao Carlos, Brazil

### Corresponding author:

Jeroen JJP van den Beucken, Radboud UMC, Philips van Leydenlaan 25, Nijmegen 6500 HB, The Netherlands.

Email: jeroen.vandenbeucken@radboudumc.nl

at the interface of the material which results in the formation of a bond between the bone tissue and the material.<sup>7,8</sup>

Generally, CaPs are used as monolithic, biphasic, triphasic, or multiphasic formulations to obtain an appropriate balance between thermodynamically stable and soluble CaP phases.<sup>9,10</sup> In this respect, hydroxyapatite (HA) is more stable under physiological conditions and has slower resorption kinetics compared to tricalcium phosphate (TCP). On the other hand, the higher biodegradability of TCP enhances the reactivity of biphasic formulations based on HA and TCP by increasing TCP/HA ratio. In general, biphasic, triphasic, or multiphasic CaPs have the advantage of using the more soluble/less soluble ratio by preferential dissolution of the more soluble CaP components.<sup>4</sup>

In addition to CaP, BGs are considered appealing implant materials for bone-related applications. These BGs comprise a group of silica-based melt-derived glasses with a unique ability to promptly bond to bone tissue and in addition stimulate progenitor cells toward increased mineralized matrix deposition.<sup>11</sup> Biosilicate<sup>®</sup> is a BGC based on the  $P_2O_5$ - $Na_2O$ - $CaO$ - $SiO_2$  system and obtained by controlled crystallization.<sup>12</sup> In vitro studies with Biosilicate<sup>®</sup> have demonstrated surface nucleation and growth of apatitic crystals upon immersion in simulated body fluid (SBF) and larger areas of calcified matrix compared to Bioglass<sup>®</sup> 45S5 at day 17 of osteogenic cell culture.<sup>13,14</sup> In addition, in vivo studies with rats indicated higher bone formation and increased mechanical strength of tibial defects treated with Biosilicate<sup>®</sup> compared to the control group without filler particles.<sup>12,15</sup>

Despite the bioactivity of CaPs and BGs, these materials are primarily available as powder and monoliths; thus their handling properties should be further optimized in terms of cohesive moldability to improve filling of defects of complex geometry.<sup>16</sup> In more detail, progress made in improving handling properties of ceramic granulate can be used, where polymeric carriers have been reported to render putty-like materials without affecting the biological performance of the granulate ceramic.<sup>17,18</sup> Barbieri et al.<sup>17</sup> showed superior bone forming potential of carboxymethyl cellulose (CMC)-based ceramics putties compared to other polymeric carrier formulations. More recently, a putty-like material based on carboxymethylcellulose-glycerol (CMCG) and ceramic granulate was developed to overcome the disadvantage of carriers containing water, which may degrade the surface microstructure of granulate ceramic, which subsequently might affect bone responses. The water-free CMCG carrier demonstrated superior in vitro and in vivo performance in terms of preserving the chemistry, microstructure, and performance of osteoinductive CaP ceramic.<sup>18</sup> At the

same time, CMCG offered a range of handling properties from moldable putty to flowable paste, depending on TCP particle sizes and wt% of CMCG.<sup>18</sup>

Toward optimization of the handling properties of ceramic granulate, this study evaluated the handling (i.e. cohesion), physicochemical features, and morphological characteristics of formulations consisting of CMCG carriers containing either hydroxyapatite-tricalcium phosphate (HA-TCP) or Biosilicate<sup>®</sup> granules. We hypothesized that both materials, HA-TCP and Biosilicate<sup>®</sup>, would have superior handling properties when combined with CMCG, mainly by exploiting the moldability of this polymeric carrier with the bioactivity of the ceramic granulate. In addition to characterization of the microstructure, cohesion, mineralization, pH, and viscoelastic properties of the novel formulations, cell culture experiments were performed to investigate (i) the cytotoxicity of the new formulations and (ii) the influence of the formulations on cell proliferation.

## Materials and methods

### Materials

CMC was provided by CP Kelco (MW = 50,000, CeKol, Nijmegen, The Netherlands) and glycerol ultrapure by Sigma-Aldrich (Zwijndrecht, The Netherlands). HA-TCP (60–40%, in composition respectively), particle size 425–500  $\mu\text{m}$ , was produced and provided by CAM Bioceramics (Leiden, The Netherlands). Biosilicate<sup>®</sup>, particle size 250–1000  $\mu\text{m}$ , was provided by Vitreous Materials Laboratory (LaMaV; Department of Materials Engineering, Federal University of São Carlos, São Carlos, São Paulo, Brazil). Biosilicate<sup>®</sup> was obtained from fully crystallized glass ceramics of the  $Na_2O$ - $CaO$ - $SiO_2$ - $P_2O_5$  system, by double stage thermal treatment.<sup>19</sup>

### Preparation of HA-TCP/CMCG and Biosilicate<sup>®</sup>/CMCG formulations

CMC was dissolved in glycerol (5% w/w) at 95°C, after which either HA-TCP or Biosilicate<sup>®</sup> granulate was added at different ratios (Table 1) with the aim to maximize the ceramic content for a moldable formulation according to previously described methods.<sup>18</sup> Briefly, granulate was combined with the polymeric carrier at different volumetric ratios for optimal handling characteristics. The granulate was mixed with a spatula until a visually homogeneous distribution of the ceramic granulate throughout the carrier was obtained, without phase separation between polymeric carrier and HA-TCP or Biosilicate<sup>®</sup>. The materials were considered as moldable due to their putty-like consistency after

**Table 1.** Composition of CMCG-ceramic granulate formulations.

Formulations	HA-TCP or Biosilicate (wt%)	CMCG (wt%)	Proportion (material:CMCG)
HA-TCP50	50	50	1.0:1.0
BGC50			
HA-TCP60	60	40	1.2:0.8
BGC60			
HA-TCP70	70	30	1.4:0.6
BGC70			
HA-TCP80	80	20	1.6:0.4
BGC80			
HA-TCP100	100	0	2.0:0.0
BGC100			

CMCG: carboxymethylcellulose–glycerol; HA-TCP: hydroxyapatite-tricalcium phosphate.

mixing<sup>18,20</sup> and they were set to dry overnight at room temperature. After preparation and at each time point (three, seven, 14, 21, and 28 days), the formulations were freeze-dried, mounted on stubs with carbon tape, and sputter coated using gold. Scanning electron microscopy (SEM; JEOL 6310) was performed to analyze the morphology of the formulations. The formulations with 100% HA-TCP or Biosilicate<sup>®</sup> (HA-TCP100 and BGC100) were utilized to check the morphological features, mineralization, cytotoxicity, and effect on DNA amount (cell culture) of both granulate ceramics without CMCG.

### *In vitro behavior of formulations in phosphate-buffered saline (PBS)*

Disintegration kinetics of the HA-TCP/CMCG and Biosilicate<sup>®</sup>/CMCG formulations were evaluated by soaking in PBS using the ratio 0.5/15 ml at 37°C in glass vials under static conditions. Disintegration was defined as the condition in which (ceramic) particles are completely dispersed at the bottom of the glass vials.<sup>17,18</sup>

### *Rheology*

The viscoelastic properties of the formulations (n=4) were evaluated using an AR2000ex rheometer (TA Instrument, New Castle, NJ, USA) with a flat steel-plate geometry (20 mm diameter) at 37°C. Storage ( $G'$ ) and loss moduli ( $G''$ ) were determined in oscillatory time sweep tests for 10 min at a gap distance of 1500  $\mu$ m by subjecting the samples to an oscillatory stress of 25.0 Pa and a frequency of 1 Hz. The obtained values were plotted as  $\tan(\delta)$  values ( $G''/G'$  ratio) for each sample.

### *Mineralization in SBF*

The mineralization capacity of HA-TCP and Biosilicate<sup>®</sup> within HA-TCP/CMCG and Biosilicate<sup>®</sup>/CMCG formulations was evaluated in vitro using the methods described by Kokubo and Takadama.<sup>21</sup> SBF having the same ionic composition as blood serum was prepared under laminar flow to prevent contamination. HA-TCP/CMCG and Biosilicate<sup>®</sup>/CMCG formulations and both granulates without polymeric carrier (0.11 ml; n=3) were placed in glass vials containing 13.20 ml of SBF (volumes calculated according to Kokubo and Takadama<sup>21</sup>) at 37°C on a shaker table (70 Hz) for up to 28 days, with refreshment on days 3, 7, 14, and 21. At each refreshment, the solution of the previous period was saved for analysis of the calcium content in SBF using the orthocresolphthalein complex-one assay.<sup>22</sup> These solutions were incubated overnight in 1 ml of 0.5 N acetic acid on a shaker table. For analysis, 300  $\mu$ l working reagent was added to 10  $\mu$ l sample or standard in a 96-well plate. The plate was incubated for 10 min at room temperature. The absorbance of each well was measured on a microplate spectrophotometer at 570 nm (Bio-Tech Instruments, Winooski, VT, USA). The standards (ranging between 0 and 100  $\mu$ g/ml) were prepared using a  $\text{CaCl}_2$  stock solution. Data were obtained from triplicate samples and measured in duplo. The depletion of Ca was plotted cumulatively by measuring the difference between the Ca concentration in the sample-free SBF control solutions and the SBF solution in the presence of HA-TCP/CMCG and Biosilicate<sup>®</sup>/CMCG formulations.<sup>23</sup> Additionally, the samples, at each time point, were retrieved, freeze-dried, sputter coated with gold, and visually evaluated by SEM (morphology after incubation).

### *pH measurements*

At each indicated time point during incubation in SBF, the pH of the SBF was measured (n=3) using a pH electrode (Meterlab PHM210 Radiometer Analytical, Villeurbanne, France).

### *Mass measurements*

For mass measurements, the formulations (0.17 ml) were placed in 5.0 ml of PBS and incubated for 1, 4, 8, 16, and 24 h at 37°C. After each experimental period, the formulations were retrieved from the solution and weighed. The mass gain due to swelling (weight increase accompanied by volume change) or mass loss due to dissolution was calculated using the formula

$$\text{Mass\%} = [(W_t - W_0)/W_0] \times 100\%$$

where  $W_0$  is the weight of the sample before immersion in PBS and  $W_t$  is the weight of the sample after immersion time ( $t$ ) in PBS. Measurements were performed in triplicate ( $n = 3$ ).

### Cell culture studies

The cytotoxicity of the new formulations, as well their influence on DNA amount was evaluated by an indirect assay, using material extracts, as described previously.<sup>24</sup> The use of materials extracts, for testing biomaterials and medical devices, is in accordance with ISO 10993-5 standards related to standardization of cytotoxicity tests.<sup>25,26</sup> Briefly, after preparation followed by sterilization in 70% ethanol,<sup>24</sup> all formulations (0.06 ml;  $n = 4$ ) were put in contact with 2 ml of cell culture medium (alpha Minimal Essential Medium without ascorbic acid;  $\alpha$ -MEM; Gibco BRL, Life Technologies, Breda, The Netherlands) supplemented with 10% fetal bovine serum (FBS; Gibco) and 1% p/s (penicillin/streptomycin; Gibco) for one, three, and seven days. As controls, four empty wells were filled with the same amount of medium for each time point.

MC3T3-E1 subclone cells (ATCC CRL-2593) from passage 27<sup>27</sup> were cultured in proliferation medium containing  $\alpha$ -MEM (Gibco) supplemented with 10% FBS (Gibco) and 50  $\mu$ l/ml gentamicin (Gibco) in a humidified incubator set at 37°C and 5% CO<sub>2</sub>. Upon 80% confluency, cells were detached using trypsin/EDTA and seeded at a density of  $4 \times 10^4$  cells/cm<sup>2</sup> in 48-well plates containing 500  $\mu$ l of medium. After overnight incubation, the medium was changed for the pre-conditioned medium that was previously collected and the cells were incubated for three days. Afterward, the alamarBlue<sup>®</sup> assay (Bio-Rad AbD Serotec GmbH, Puchheim, Germany) was used on all samples to determine cell viability. For analysis, 500  $\mu$ l of alamarBlue<sup>®</sup> solution was added to each well, and the plate was stored in the dark for 4 h at 37°C in a cell culture incubator. After this period, the samples were transferred to a 96-well plate. Measurement was performed using a microplate reader (Bio-Tek Instruments, Inc.) at 570 nm.

Subsequently, the alamarBlue<sup>®</sup> solution in contact with cells was washed away twice using PBS and the same well plate was used for DNA quantification by PicoGreen assay (QuantiFluor<sup>®</sup> dsDNA quantification kit; Promega, Leiden, The Netherlands). After two freeze-thaw cycles (−80°C and 20°C), 100  $\mu$ l of freshly made working solution was added into each well which contained 100  $\mu$ l of sample or DNA standard, and the plate was stored in the dark for 5 min. Finally, the fluorescent signal (485/20 excitation and 528/20 emission) was read using a microplate reader (Bio-Tek Instruments, Inc.).

### Statistical analysis

Data were expressed as mean  $\pm$  standard deviation. Statistical analyses were performed using STATISTICA 7.0 (StatSoft Inc., Oklahoma, USA). Shapiro–Wilk normality test was used to check distribution. Kruskal–Wallis test and Dunn post hoc were used for nonparametric data. One-way analysis of variance and Tukey–Kramer multiple comparisons posttests were used for parametric data. Differences were considered significant at  $p \leq 0.05$ .

## Results

### *In vitro* behavior in PBS

Evaluation of the *in vitro* behavior showed that the compositions with 80% of either HA-TCP or Biosilicate<sup>®</sup> (HA-TCP80 and BGC80, respectively) were not cohesive and disintegrated immediately upon immersion in PBS. The other putty-like formulations required longer than 72 h for disintegration. Based on these observations demonstrating limited cohesive properties, the formulations HA-TCP80 and BGC80 were not used for further analyses.

### *Morphology before incubation in SBF*

After preparation, all formulations containing either HA-TCP or Biosilicate<sup>®</sup> combined with CMCG exhibited a putty-like appearance. SEM micrographs indicated that the granulates were well aggregated by the CMCG-based mesh (Figure 1). The CMCG-based mesh could be seen covering and connecting the particles. The moldable formulations (HA-TCP50, BGC50, HA-TCP60, and BGC60) were easy to handle without loss of particles. The HA-TCP70 and BGC70 formulations were more difficult to shape, and a few ceramic particles were lost from the masses upon handling.

### Rheology

Figure 2 shows the viscoelastic properties of the different formulations. The highest  $\tan(\delta)$  values were observed for the compositions HA-TCP50, BGC50, and BGC60 (ranging between 0.51 and 0.60), with statistical difference between BGC60 and BGC50 ( $p = 0.005$ ). The formulations HA-TCP60, HA-TCP70, and BGC70 had statistically lower  $\tan(\delta)$  values ( $0.08 \pm 0.03$ ) compared to the other groups ( $p = 0.0002$ ), indicating a predominantly elastic behavior for these putties. A significant statistical difference was also found for HA-TCP70 compared to HA-TCP60 ( $p = 0.05$ , Figure 2).

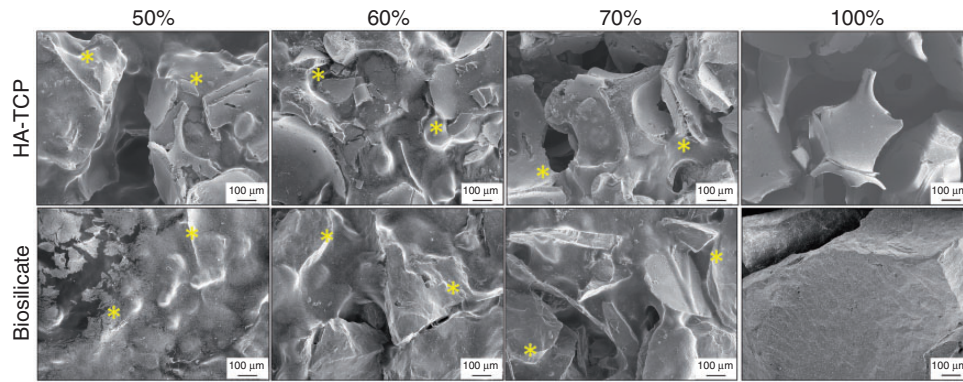


**Figure 1.** SEM micrographs of the different formulations at day 0 (after preparation). Asterisks indicate CMCG-based mesh. 100 $\times$  magnification. CMCG: carboxymethylcellulose–glycerol; SEM: scanning electron microscopy.

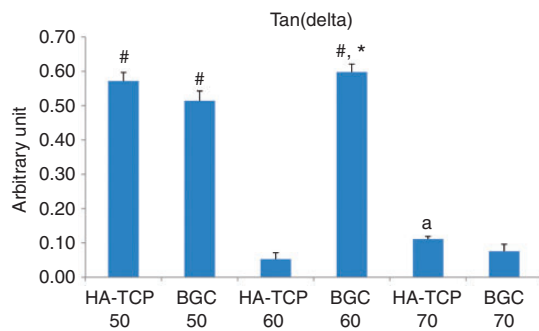


**Figure 2.** Tan( $\delta$ ) values of the HA-TCP/CMCG and Biosilicate<sup>®</sup>/CMCG putties. #—HA-TCP50, BGC50, and BGC60 compared to HA-TCP60, HA-TCP70, and BGC70 ( $p = 0.0002$ ); \*—BGC60 compared to Group BGC50 ( $p = 0.005$ ); a—Group HA-TCP70 compared to HA-TCP60 ( $p = 0.05$ ). CMCG: carboxymethylcellulose–glycerol; HA-TCP: hydroxyapatite–tricalcium phosphate.

### Mineralization in SBF

Among the HA-TCP/CMCG formulations (Figure 3(a)), the mineralization was statistically higher for HA-TCP60 ( $\sim 1.1$  mg;  $p = 0.02$ ) and HA-TCP70 ( $\sim 1.2$  mg;  $p = 0.002$ ) compared to HA-TCP100 ( $\sim 0.8$  mg) at day 10. From day 14 until day 28 statistical differences were found in HA-TCP100 (lower amount of calcium uptake compared to all other formulations;  $0.0003 < p < 0.03$ ). Specifically, after 14 days of immersion, values for HA-TCP70 ( $\sim 1.8$  mg) were significantly higher compared to HA-TCP50 ( $\sim 1.1$  mg;  $p = 0.03$ ). During 28 days of SBF immersion, the mineralization studies indicated for all HA-TCP/CMCG formulations a continuous increase in calcium uptake, reaching maximum values ranging from approximately 0.1 to 3.4 mg (Figure 3(a)).

Among Biosilicate<sup>®</sup> formulations (Figure 3(b)), BGC50 showed an initial release of calcium into the medium at day 3 ( $-0.1$  mg), being statistically lower

compared to the other groups ( $\sim 0.2 \pm 0.1$  mg;  $0.0001 < p < 0.05$ ). After seven days of immersion, the formulation BGC100 showed a significantly higher cumulative Ca uptake ( $\sim 0.6$  mg) compared to BGC60 ( $\sim 0.4$  mg;  $p = 0.04$ ). For the remainder of the incubation period, no statistical differences were found among Biosilicate<sup>®</sup>/CMCG formulations ( $p > 0.05$ ; Figure 3(b)). During 28 days of SBF incubation, all Biosilicate<sup>®</sup>/CMCG formulations showed a continuous increase in Ca uptake, reaching values ranging from approximately  $-0.08$  to 3.0 mg (Figure 3(b)).

### pH measurements

HA-TCP/CMCG formulations showed a relatively constant pH value over time, with variations between 7.2 and 7.5 (Figure 4(a)). Statistical differences were observed after 28 days of immersion, when a higher pH value was observed for HA-TCP100 compared to HA-TCP50 ( $p = 0.0002$ ), HA-TCP60 ( $p = 0.0002$ ), and HA-TCP70 ( $p = 0.0136$ ). Additionally, at day 28, the pH for HA-TCP60 was significantly lower compared to HA-TCP70 ( $p = 0.0043$ ; Figure 4(a)).

In general, Biosilicate<sup>®</sup>/CMCG formulations displayed pH values ranging between 7.4 and 7.9 (Figure 4(b)). The formulation BGC100 showed a higher pH ( $\sim 7.8$ ) compared to the other formulations ( $7.62 \pm 0.01$ ) at day 3 ( $p = 0.0002$ ). A pH increase was observed for Biosilicate<sup>®</sup>/CMCG-based formulations until day 7, after which a plateau was reached. After day 21, all formulations revealed a pH decrease, with significant lower values for BGC50 comparing to the other formulations (Figure 4(b);  $p = 0.0002$ ).

### Mass measurements

Mass measurements were performed to investigate the cohesion and weight gain/loss of the different formulations upon soaking in PBS (Figure 5). HA-TCP/

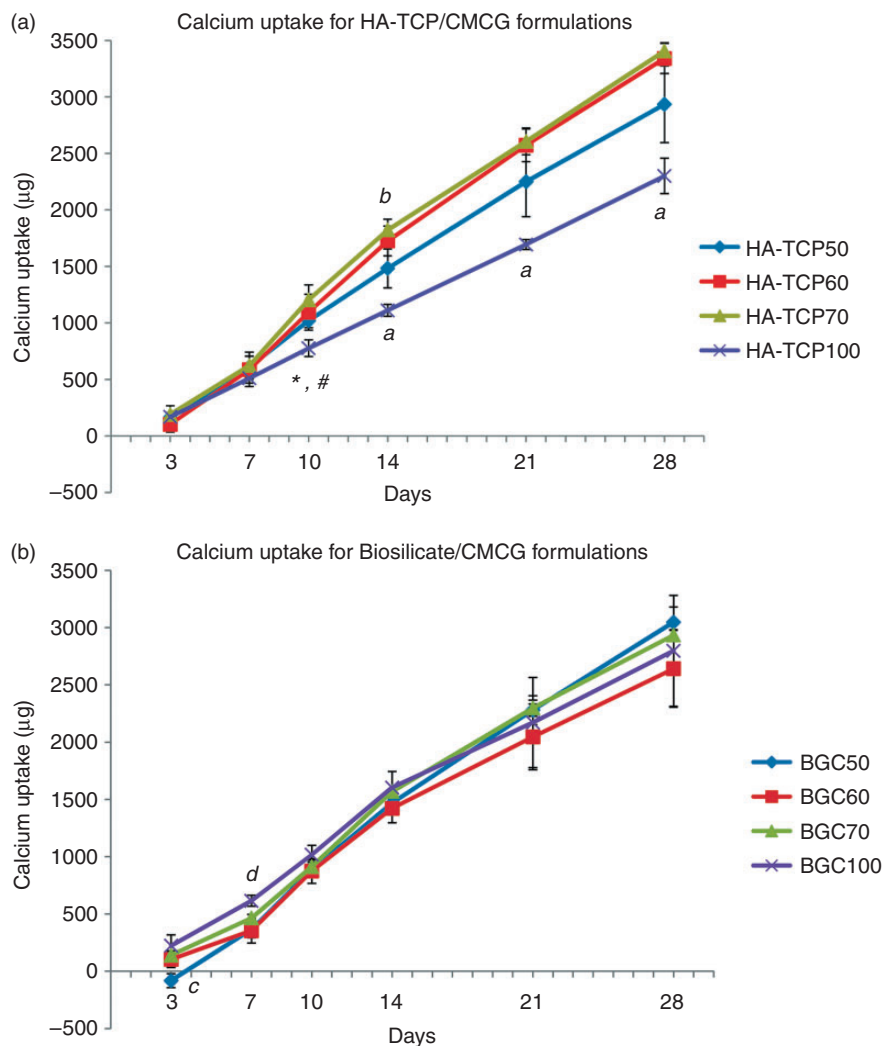


**Figure 3.** Cumulative calcium uptake by (a) HA-TCP/CMCG and (b) Biosilicate<sup>®</sup>/CMCG formulations in SBF for up to 28 days. \*—HA-TCP70 compared to HA-TCP100 ( $p = 0.002$ ); #—HA-TCP60 compared to HA-TCP100 ( $p = 0.02$ ); a—HA-TCP100 compared to all other groups ( $0.0003 < p < 0.03$ ); b—HA-TCP70 compared to HA-TCP50 ( $p = 0.03$ ); c—BGC50 compared to all other groups ( $0.0001 < p < 0.05$ ); d—BGC100 compared to BGC60 ( $p = 0.04$ ). CMCG: carboxymethylcellulose–glycerol; HA-TCP: hydroxyapatite-tricalcium phosphate.

CMCG formulations exhibited an intense swelling (between ~80 and 100%) after 1 h. This event continued until the last time point (i.e. 24 h), reaching the approximate values of 180, 136, and 126% for HA-TCP50, HA-TCP70, and HA-TCP60, respectively. For all experimental periods, HA-TCP50 swelling values were statistically higher compared to the other groups (Figure 5(a);  $0.0004 < p < 0.03$ ). This fact indicates that swelling increases for HA-TCP/CMCG formulations with increasing amounts of the polymer.

After 1 h of immersion in PBS, all Biosilicate<sup>®</sup>/CMCG formulations showed an evident swelling, leading to an increase in their original mass (BGC50 ~72, BGC60 ~67, and BGC70 ~48%; Figure 5(b)). At 16 h of incubation, the swelling

values were  $128 \pm 7\%$  for BGC50 and BGC60, being statistically higher compared to BGC70 (90%;  $p = 0.046$  and  $0.0074$ , respectively). Thereafter, the BGC50 formulation reached a plateau, whereas BGC60 and BGC70 started losing their mass, without collapsing. After 24 h of immersion, the mass increase for BGC50 (~130%) was significantly higher compared to that of BGC70 (~70%;  $p = 0.0068$ ). The mass measurements indicated that swelling increases for Biosilicate<sup>®</sup>/CMCG formulations with increasing amounts of the polymer.

### Morphology after incubation in SBF

SEM micrographs indicated degradation of the HA-TCP/CMCG and Biosilicate<sup>®</sup>/CMCG formulations

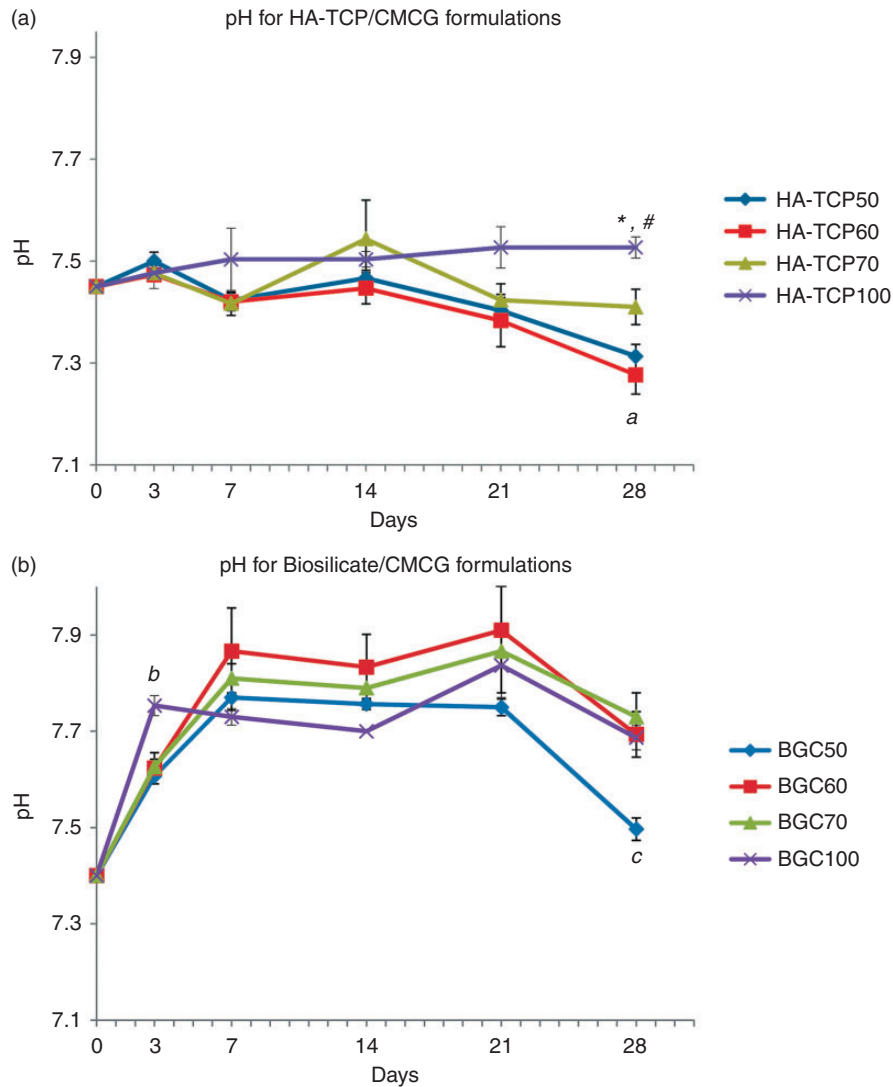


**Figure 4.** pH of SBF solution in contact with (a) HA-TCP and (b) Biosilicate® formulations for up to 28 days. \*—HA-TCP100 compared to HA-TCP50 and HA-TCP60 ( $p = 0.0002$ ); #—HA-TCP 100 compared to HA-TCP 70 ( $p = 0.0136$ ); a—HA-TCP 60 compared to HA-TCP 70 ( $p = 0.0043$ ); b—BGC 100 compared to all other groups ( $p = 0.0002$ ); c—BGC 50 compared to all other groups ( $p = 0.0002$ ). HA-TCP: hydroxyapatite-tricalcium phosphate.

overtime, being most evident at day 28 (Figure 6). The degradation was influenced by CMCG at all time points, since this process was more pronounced for the composite formulations compared to the materials not combined with CMCG—HA-TCP100 and BGC100 (Figure 6(a) and (c)). Although degradation was observed, higher magnification clearly showed preservation of the microstructure of both materials (Figure 6(b) and (d)).

### Cell culture studies

Cytotoxicity studies using alamarBlue® indicated that all preconditioned medium obtained from immersing formulations did not affect cell viability, since

no statistical difference was found among groups (Figure 7(a.1) to (a.3);  $p > 0.05$ ). All the materials tested showed similar values for cell viability compared to the control at each time point.

DNA quantification by PicoGreen assay indicated no significant difference among groups for the preconditioned media obtained after one day (Figure 7(b.1)). On the other hand, the preincubated medium with HA-TCP60 for three days led to an increased amount of DNA compared to control group (Figure 7(b.2);  $p = 0.0036$ ). Moreover, at the last time point, statistically higher values of DNA were noticed for BGC50 (~904 ng) and HA-TCP60 (~1092 ng) compared to control group (~216 ng) and BGC100 (~122 ng) (Figure 7(b.3);  $0.0003 < p < 0.03$ ).

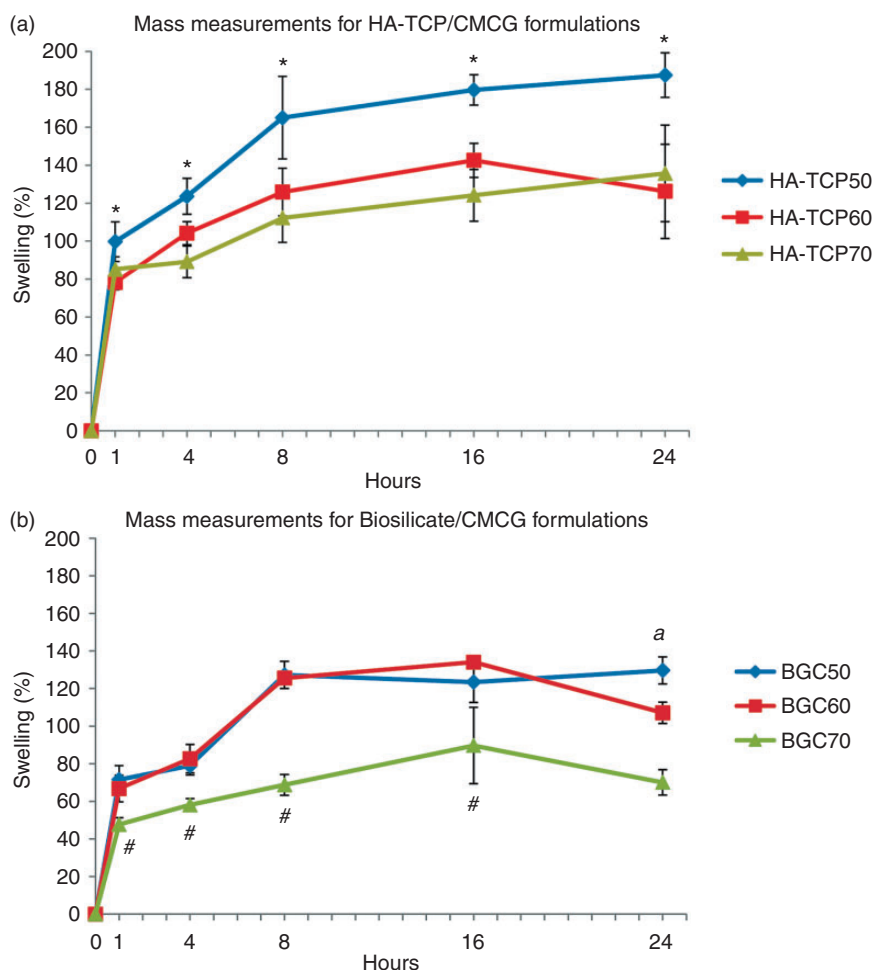


**Figure 5.** Swelling of (a) HA-TCP/CMCG and (b) Biosilicate<sup>®</sup>/CMCG formulations in PBS for up to 24 h. \*—HA-TCP50 compared to all other groups ( $0.0004 < p < 0.03$ ); #—BGC70 compared to all other groups ( $0.0009 < p < 0.02$ ); a—BGC50 compared to BGC70 ( $p = 0.0068$ ). CMCG: carboxymethylcellulose–glycerol; HA-TCP: hydroxyapatite–tricalcium phosphate.

## Discussion

To improve handling properties of particulate bioceramic materials, this study evaluated the properties of formulations composed of either HA-TCP or Biosilicate<sup>®</sup> combined with CMCG. For this, in vitro dissolution (cohesion), rheology, Ca uptake, and degradability were studied. The hypothesis was that both ceramic materials—HA-TCP and Biosilicate<sup>®</sup>—in combination with CMCG would have superior handling properties and cohesion compared to the plain ceramics. The results showed that mixing these ceramic materials with CMCG generates putty-like formulations with improved cohesion and moldability compared to the granular ceramics. Interestingly, the composite formulations exhibited a continuously increasing mineralization upon incubation in SBF. Remarkably, mineralization of HA-TCP/CMCG formulations was enhanced compared to pure HA-TCP. Additionally, cell culture experiments

showed that all formulations were devoid of cytotoxic effects and that HA-TCP60 and BGC50 extracts led to an increased cell proliferation compared to the control group and BGC100.

The formulations were maximized with respect to their HA-TCP and Biosilicate<sup>®</sup> content to obtain the maximum amount of the bioactive materials without affecting cohesion<sup>28,29</sup> and moldability.<sup>30,31</sup> The highest possible amount of HA-TCP or Biosilicate<sup>®</sup> was found to be 70 wt%, and the formulations were still cohesive. For composite formulations with higher amounts of ceramic material (i.e. 80 and 90 wt%), loss of cohesion was observed. Additionally, formulations containing less than 50 wt% ceramic were not evaluated, since they consisted of nonhomogeneous compositions. All composite formulations were moldable unlike pure HA-TCP (HA-TCP100) and Biosilicate<sup>®</sup> (BGC100). Moldable bone substitutes have several advantages over granules/powder or preset scaffolds/disks, including a superior handling in a surgical setting, improved

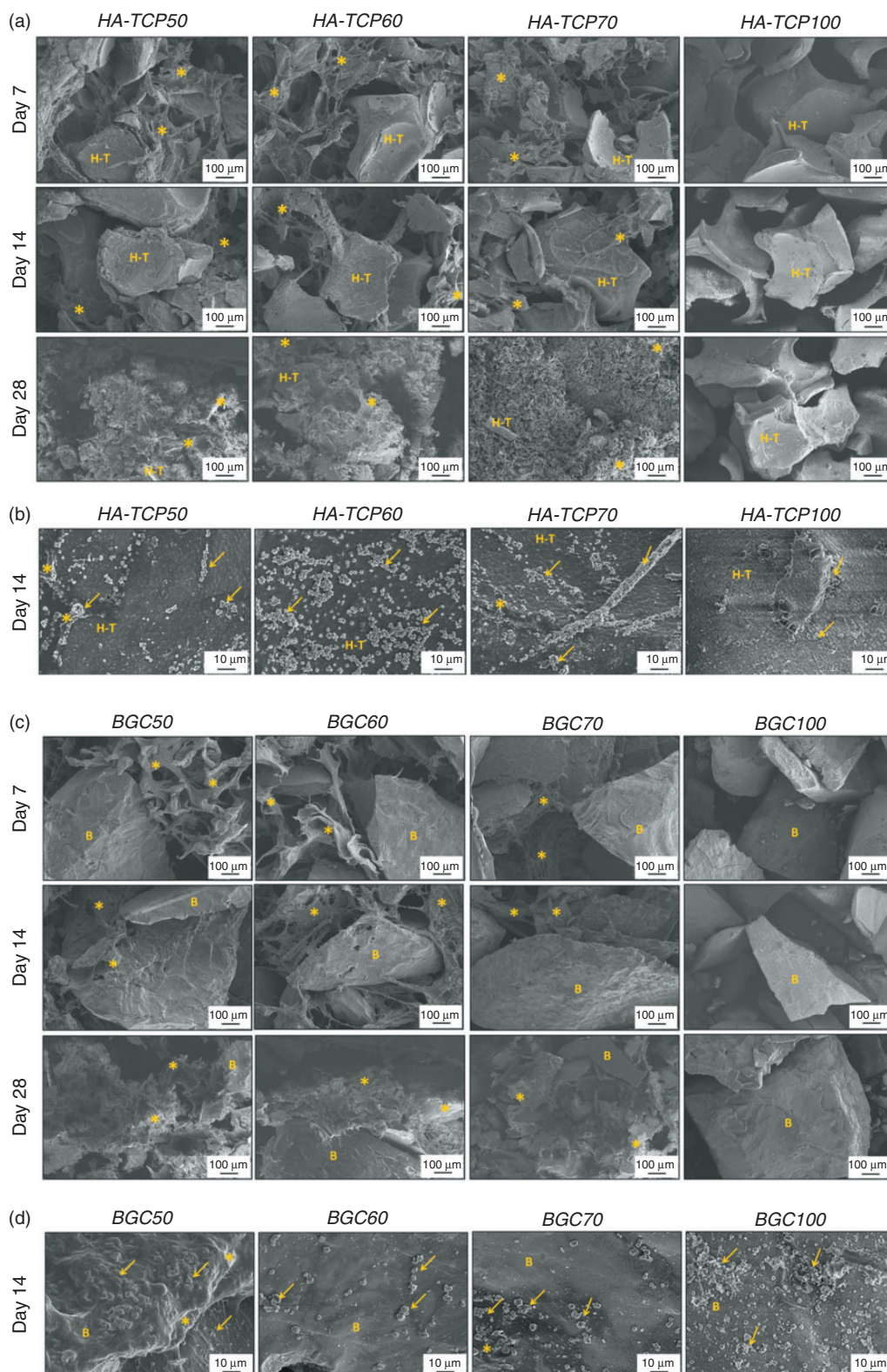


**Figure 6.** SEM micrographs of the different formulations after seven, 14, and 28 days of incubation in SBF. (a) HA-TCP formulations, 100× magnification; (b) HA-TCP formulations at day 14, 1000× magnification; (c) Biosilicate® formulations, 100× magnification; and (d) Biosilicate® formulations at day 14, 1000× magnification. H-T: HA-TCP; \*: CMCG; →: CaP; B: Biosilicate®. CMCG: carboxymethylcellulose-glycerol; HA-TCP: hydroxyapatite-tricalcium phosphate.

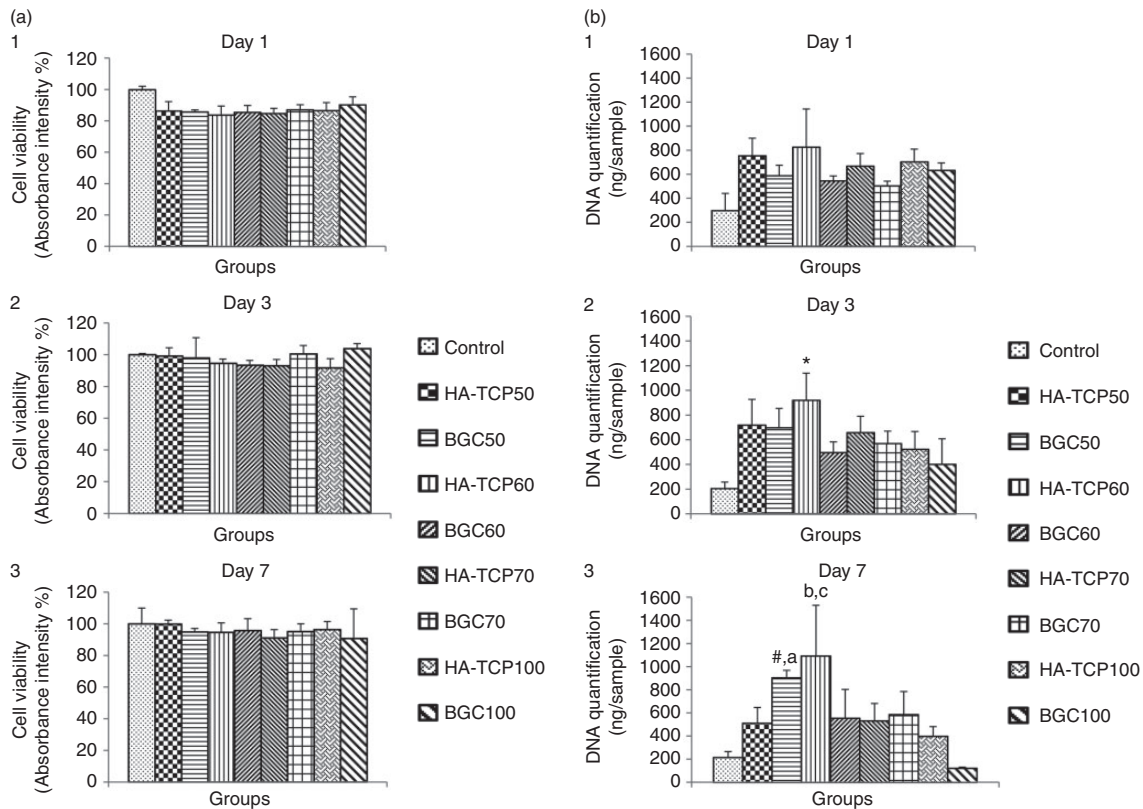


**Figure 7.** Cell viability (a) and DNA quantification (b) for MC3T3-E1 cells in contact with preconditioned medium obtained one, three, and seven days after immersing the different formulations in  $\alpha$ -MEM. (a)1 and (b)1; (a)2 and b(2); and a(3) and b(3) represent day 1, day 3, and day 7, respectively. \*—HA-TCP60 compared to control (0.0036); # and a—BGC50 compared to control ( $p = 0.0287$ ) and BGC100 (0.0036), respectively; b and c—HA-TCP60 compared to control ( $p = 0.0254$ ) and BGC100 (0.0031), respectively. HA-TCP: hydroxyapatite-tricalcium phosphate.

shape conformance to complex bone defects, and retention within such bone defects.<sup>18,30,32</sup>

All moldable composite formulations required more than 72 h for in vitro disintegration. In contrast to that, Barbieri et al.<sup>17</sup> showed that HA-TCP/CMC putties needed only 24 h for dissolution and Davison et al.<sup>18</sup> reported that TCP/CMCG putties required 48 h for complete dissolution. This difference may be related to the interactions of either HA or Biosilicate<sup>®</sup> with CMCG,<sup>23,33–35</sup> giving rise to a more stable material,<sup>36</sup> but not stiffer, allowing significant swelling and, at the same time, preventing disintegration of the composite formulations. Furthermore, rheology studies indicated that all formulations formed gels with elastic-like behavior as reflected by the values for  $\tan(\delta)$  which were all lower than 1,<sup>37</sup> which can be attributed to the CMCG gel-forming ability.<sup>17,36</sup>

For all composite formulations, the mineralization assay in SBF indicated a continuous uptake of Ca during 28 days of incubation. Interestingly, SEM micrographs indicated the precipitation of CaP on the composite surface. These facts may be related to the formation of an HA-like layer on the surface of

the two materials, a phenomenon well known for biomaterials similar to the ones used here.<sup>38–42</sup>

These leaching reactions are well established for this kind of materials and are defined by Hench as five-stage reactions.<sup>43</sup> Briefly, in stage I, alkali and alkali earth ions are released from the material into the fluid and replaced by  $H^+$  or  $H_3O^+$  ions in the ceramic structure. This reaction raises the local pH, resulting in the break of Si–O–Si bonds. Then, in stage II, silicon is released into the fluid in the form of silanol groups ( $Si(OH)_4$ ). In stage III, the silanols condense, forming a polymerized silica gel layer on the surface of the material. Afterward, in stage IV, calcium and phosphate ions that had diffused from the material or from the fluid form an amorphous calcium phosphate layer over the silica gel. Subsequently to these reactions, in stage V, the amorphous calcium phosphate layer integrates the carbonate species and crystallizes into HCA.<sup>43</sup>

In this study, most probably, the HA crystals could be better observed using magnifications higher than 1000X. Additionally, the freeze-drying process after incubation could have led to the (partial) detachment of the HA layer from the surface of the particles. Based

on our observations, further studies should utilize higher magnifications and different postincubation treatments in order to increase the quality of SEM analysis toward the visualization of the formed HA crystals. HA-TCP/CMCG formulations showed a higher mineralization capacity compared to pure HA-TCP (HA-TCP100). Differently, the Biosilicate<sup>®</sup>/CMCG formulations did not mineralize more pronounced compared to pure Biosilicate<sup>®</sup> (BGC100). This difference may likely be related to the differences in particle size for HA-TCP (425–500  $\mu\text{m}$ ) and Biosilicate<sup>®</sup> (250–1000  $\mu\text{m}$ ) and the related specific surface area. HA-TCP smaller particles—with higher surface area—could be in closer contact with CMCG, allowing a greater protection of the biomaterial microstructure, thereby retaining its bioactivity to a higher extent. Indeed, the preservation of the microstructure of HA-TCP and Biosilicate<sup>®</sup> was observed by SEM micrographs after each incubation period and corroborates the observations made by Davison et al.<sup>18</sup> who observed preservation of surface microstructure and performance of osteoinductive CaP ceramics in water-free carriers.<sup>18</sup>

The pH measurements indicated that CMCG prevented substantial variation of this parameter for all formulations, partially neutralizing it. Accordingly, Davison et al.<sup>18</sup> reported the pH of water-free carriers combined with TCP to be near neutral. In contrast, Gabbai-Armelin et al.<sup>23</sup> showed that incorporation of Biosilicate<sup>®</sup> into alginate resulted in alkalinization of the medium (pH  $\sim$ 10 in the first day). This dissimilarity may especially be due to the smaller Biosilicate<sup>®</sup> particle size (2.5  $\mu\text{m}$ ) utilized in the latter work, leading to a faster dissolution/degradation, releasing ions (Si, Na, Ca, and  $\text{PO}_4^{3-}$ ) and, consequently, inducing an increase in pH.<sup>23,44</sup>

Mass measurements indicated swelling for all the formulations upon immersion in PBS. Possibly, water absorption into the polymer led to an increase in the original mass, but the formulations were still cohesive. In physiological solutions, CMC swells and could conceivably absorb critical nutrients and growth factors, as well fill any bone voids.<sup>18,45,46</sup> On the other hand, the remarkable swelling exhibited by the formulations, especially by the HA-TCP/CMCG combinations, may also cause problems upon implantation in defects (affecting the adjustment of the biomaterial into the site), and this fact should be addressed in more detail by further *in vivo* studies.

To study the possible cytotoxicity of the new formulations, as well their influence on cell proliferation, an indirect method was used by culturing MC3T3 cells in preconditioned medium. The results showed that neither formulation was cytotoxic to the cells. It was assumed that the well-established leaching reactions,<sup>43</sup> leading to ionic release from the materials, did not

provoke harmful effects to the cells which were capable of surviving and proliferating. Interestingly, PicoGreen assay indicated increased amounts of DNA for preconditioned media compared to control medium, especially for BGC50 and HA-TCP60 formulation after seven days of incubation. It is suggested that the biomaterials extracts created a favorable microenvironment<sup>47,48</sup> which induced cell proliferation. This fact may be pivotal toward the healing of damaged tissue, since cell proliferation is required to the replacement of dead cells and lost structures.<sup>49,50</sup> Further cell culture studies should focus on direct contact of the cells with the present composites, as well as on analyzing osteogenic marker expressions at relevant time points.

In summary, the present results justify additional cell culture and preclinical *in vivo* studies on HA-TCP/CMCG and Biosilicate<sup>®</sup>/CMCG to evaluate and validate the osteogenic potential, histocompatibility, and biological performance of these materials for bone regeneration and augmentation purposes.

## Conclusions

Based on our experimental data on novel formulations containing CMCG + HA-TCP or CMCG + Biosilicate<sup>®</sup>, we conclude that CMCG combined with either HA-TCP or Biosilicate<sup>®</sup> (i) allows for the generation of moldable putties for bone regeneration, (ii) improves handling properties, and (iii) retains the bioactivity of the ceramic component. Additionally, *in vitro* investigations indicated that all formulations were noncytotoxic and that HA-TCP60 and BGC50 extracts led to an increased cell proliferation, and such formulations are good candidates for future studies. Our findings justify further research focused on the biological performance of these formulations.

## Acknowledgements

PRGA thanks MSc. Luis A. B. Ferreira for supporting the production of the graphical abstract. The authors also thank Martijn Martens for assistance with scanning electron microscopy performed at the Microscopic Imaging Center (MIC) of Radboud Institute for Molecular Life Sciences (RIMLS), Nijmegen, The Netherlands.

## Declaration of Conflicting Interests

The author(s) declared no potential conflicts of interest with respect to the research, authorship, and/or publication of this article.

## Funding

The author(s) disclosed receipt of the following financial support for the research, authorship, and/or publication of this article: PRGA acknowledges the Conselho Nacional de Desenvolvimento Científico e Tecnológico (CNPq) and

Fundação de Amparo a Pesquisa do Estado de São Paulo (FAPESP) for the scholarships (grants no. 209507/2013-6 and 2015/20704-8, respectively).

## References

1. Tonetti MS, Hammerle CH and European Workshop on Periodontology Group C. Advances in bone augmentation to enable dental implant placement: Consensus Report of the Sixth European Workshop on Periodontology. *J Clin Periodontol* 2008; 35: 168–172.
2. Erdogan O, Shafer DM, Taxel P, et al. A review of the association between osteoporosis and alveolar ridge augmentation. *Oral Surg Oral Med Oral Pathol Oral Radiol Endod* 2007; 104: 738.e1–13.
3. Sepulveda P, Jones JR and Hench LL. Bioactive sol-gel foams for tissue repair. *J Biomed Mater Res* 2002; 59: 340–348.
4. Dorozhkin SV. Biphasic, triphasic and multiphasic calcium orthophosphates. *Acta Biomater* 2012; 8: 963–977.
5. Jones JR. Review of bioactive glass: from Hench to hybrids. *Acta Biomater* 2013; 9: 4457–4486.
6. Lin B, Zhou H, Leaman DW, et al. Sustained release of small molecules from carbon nanotube-reinforced monite calcium phosphate cement. *Mater Sci Eng C* 2014; 43: 92–96.
7. Hench LL and Kokubo T. Properties of bioactive glasses and glass-ceramics. In: Black J and Hastings G (eds) *Handbook of biomaterial properties*. New York: Springer US, 1998, pp.355–363.
8. Hench LL. The story of Bioglass®. *J Mater Sci Mater Med* 2006; 17: 967–978.
9. Daculsi G. Biphasic calcium phosphate concept applied to artificial bone, implant coating and injectable bone substitute. *Biomaterials* 1998; 19: 1473–1478.
10. Lobo SE and Arinze LT. Biphasic calcium phosphate ceramics for bone regeneration and tissue engineering applications. *Materials* 2010; 3: 815–826.
11. Rahaman MN, Day DE, Bal BS, et al. Bioactive glass in tissue engineering. *Acta Biomater* 2011; 7: 2355–2373.
12. Bossini PS, Renno AC, Ribeiro DA, et al. Biosilicate(R) and low-level laser therapy improve bone repair in osteoporotic rats. *J Tissue Eng Regen Med* 2011; 5: 229–237.
13. Moura J, Teixeira LN, Ravagnani C, et al. In vitro osteogenesis on a highly bioactive glass-ceramic (Biosilicate). *J Biomed Mater Res Part A* 2007; 82: 545–557.
14. Crovace MC, Souza MT, Chinaglia CR, et al. Biosilicate® – a multipurpose, highly bioactive glass-ceramic. In vitro, in vivo and clinical trials. *J Non-Cryst Solids* 2016; 432: 90–110.
15. Granito RN, Renno AC, Ravagnani C, et al. In vivo biological performance of a novel highly bioactive glass-ceramic (Biosilicate(R)): a biomechanical and histomorphometric study in rat tibial defects. *J Biomed Mater Res Part B Appl Biomater* 2011; 97: 139–147.
16. Baldini N, De Sanctis M and Ferrari M. Deproteinized bovine bone in periodontal and implant surgery. *Dental Mater* 2011; 27: 61–70.
17. Barbieri D, Yuan H, de Groot F, et al. Influence of different polymeric gels on the ectopic bone forming ability of an osteoinductive biphasic calcium phosphate ceramic. *Acta Biomater* 2011; 7: 200–2014.
18. Davison N, Yuan H, de Bruijn JD, et al. In vivo performance of microstructured calcium phosphate formulated in novel water-free carriers. *Acta Biomater* 2012; 8: 2759–2769.
19. Roriz VM, Rosa AL, Peitl O, et al. Efficacy of a bioactive glass-ceramic (Biosilicate) in the maintenance of alveolar ridges and in osseointegration of titanium implants. *Clin Oral Implants Res* 2010; 21: 148–155.
20. Liu H, Li H, Cheng W, et al. Novel injectable calcium phosphate/chitosan composites for bone substitute materials. *Acta Biomater* 2006; 2: 557–565.
21. Kokubo T and Takadama H. How useful is SBF in predicting in vivo bone bioactivity? *Biomaterials* 2006; 27: 2907–2915.
22. Mooren RE, Hendriks EJ, van den Beucken JJ, et al. The effect of platelet-rich plasma in vitro on primary cells: rat osteoblast-like cells and human endothelial cells. *Tissue Eng Part A* 2010; 16: 3159–3172.
23. Gabbai-Armelin PR, Cardoso DA, Zanotto ED, et al. Injectable composites based on biosilicate[registered sign] and alginate: handling and in vitro characterization. *RSC Adv* 2014; 4: 45778–45785.
24. Shin H, Quinten Ruhe P, Mikos AG, et al. In vivo bone and soft tissue response to injectable, biodegradable oligo(poly(ethylene glycol) fumarate) hydrogels. *Biomaterials* 2003; 24: 3201–3211.
25. Baek HS, Yoo JY, Rah DK, et al. Evaluation of the extraction method for the cytotoxicity testing of latex gloves. *Yonsei Med J* 2005; 46: 579–583.
26. Li W, Zhou J and Xu Y. Study of the in vitro cytotoxicity testing of medical devices. *Biomed Rep* 2015; 3: 617–620.
27. Yan XZ, Yang W, Yang F, et al. Effects of continuous passaging on mineralization of MC3T3-E1 cells with improved osteogenic culture protocol. *Tissue Eng Part C Methods* 2014; 20: 198–204.
28. Bohner M, Doebelin N and Baroud G. Theoretical and experimental approach to test the cohesion of calcium phosphate pastes. *Eur Cells Mater* 2006; 12: 26–35.
29. Bohner M. Design of ceramic-based cements and putties for bone graft substitution. *Eur Cells Mater* 2010; 20: 1–12.
30. Ishikawa K, Miyamoto Y, Takechi M, et al. Non-decay type fast-setting calcium phosphate cement: hydroxyapatite putty containing an increased amount of sodium alginate. *J Biomed Mater Res* 1997; 36: 393–399.
31. Brydone AS, Meek D and MacLaine S. Bone grafting, orthopaedic biomaterials, and the clinical need for bone engineering. *Proc IMechE, Part H: J Engineering in Medicine* 2010; 224: 1329–1343.
32. Reynolds MA, Aichelmann-Reidy ME, Kassolis JD, et al. Calcium sulfate-carboxymethylcellulose bone graft binder: histologic and morphometric evaluation in a critical size defect. *J Biomed Mater Res Part B Appl Biomater* 2007; 83: 451–458.
33. Jiang L, Li Y, Zhang L, et al. Preparation and characterization of a novel composite containing carboxymethyl

- cellulose used for bone repair. *Mater Sci Eng C* 2009; 29: 193–198.
34. Tirapelli C, Panzeri H, Soares RG, et al. A novel bioactive glass-ceramic for treating dentin hypersensitivity. *Braz Oral Res* 2010; 24: 381–387.
  35. Garai S and Sinha A. Biomimetic nanocomposites of carboxymethyl cellulose–hydroxyapatite: Novel three dimensional load bearing bone grafts. *Colloids Surf B Biointerfaces* 2014; 115: 182–190.
  36. Ke Y, Liu GS, Wang JH, et al. Preparation of carboxymethyl cellulose based microgels for cell encapsulation. *Express Polym Lett* 2014; 8: 841–849.
  37. Mezger TG. *The rheology handbook: for users of rotational and oscillatory rheometers*. Hannover: Vincentz, 2006.
  38. Rey C. Calcium phosphates for medical applications. In: Amjad Z (ed.) *Calcium phosphates in biological and industrial systems*. New York: Springer US, 1998, pp.217–251.
  39. Combes C and Rey C. Adsorption of proteins and calcium phosphate materials bioactivity. *Biomaterials* 2002; 23: 2817–2823.
  40. Hench LL and Polak JM. Third-generation biomedical materials. *Science* 2002; 295: 1014–1017.
  41. Deborah D, Wei L, Judith AR, et al. Biosilicate<sup>®</sup> – gelatine bone scaffolds by the foam replica technique: development and characterization. *Sci Technol Adv Mater* 2013; 14: 045008.
  42. Chang K-C, Chang C-C, Chen W-T, et al. Development of calcium phosphate/sulfate biphasic cement for vital pulp therapy. *Dental Mater* 2014; 30: e362–e370.
  43. Hench LL. *Introduction to bioceramics*. 2nd ed. London: Imperial College Press.
  44. Chen Q, Roether JA and Boccaccini AR. Tissue engineering scaffolds from bioactive glass and composite materials in topics in tissue engineering. In: Ashammakhi N, Reis R and Chiellini F (eds) *Topics in Tissue Engineering*. Finland: Biomaterials and Tissue Engineering Group, University of Oulu, 2008. pp.1–27. Available at: [http://www.oulu.fi/spareparts/ebook\\_topics\\_in\\_t\\_e\\_vol4/abstracts/q\\_chen.pdf](http://www.oulu.fi/spareparts/ebook_topics_in_t_e_vol4/abstracts/q_chen.pdf).
  45. Shen SQ, Fu DJ, Xu F, et al. The design and features of apatite-coated chitosan microspheres as injectable scaffold for bone tissue engineering. *Biomed Mater* 2013. Available at: <http://iopscience.iop.org/article/10.1088/1748-6041/8/2/025007/pdf>.
  46. Badami V and Ahuja B. Biosmart materials: breaking new ground in dentistry. *Sci World J* 2014; 2014: 986912.
  47. Shin H. Fabrication methods of an engineered micro-environment for analysis of cell–biomaterial interactions. *Biomaterials* 2007; 28: 126–133.
  48. Xu W, Liao X, Zhang, et al. Tissue induction, the relationship between biomaterial’s microenvironment and mesenchymal stem cell differentiation. *J Biomed Sci Eng* 2013; 6: 85–91.
  49. Krafts KP. Tissue repair: the hidden drama. *Organogenesis* 2010; 6: 225–233.
  50. Kumar V, Abbas AK, Fausto N, et al. Tissue renewal, regeneration and repair. In: Cotran RS, Robbins SL (eds) *Pathologic basis of disease*. 8th ed. Philadelphia, PA: Elsevier, 2010, pp.79–110.